Multi-view autostereoscopic projection display using rotating screen

Osman Eldes, Kaan Akşit, and Hakan Urey*

Koç University, Department of Electrical Engineering Istanbul, 34450, Turkey

**hurey@ku.edu.tr*

Abstract: A new technique for multi-view autostereoscopic projection display is proposed, and demonstrated. The technique uses two mobile projectors, a rotating retro-reflective diffuser screen, and a head-tracking camera. As two dynamic viewing slits are created at the viewer's position, the slits can track the position of the eyes by rotating the screen. The display allows a viewer to move approximately 700 *mm* along the horizontal axis, and 500 *mm* along the vertical axis with an average crosstalk below 5 %. Two screen prototypes with different diffusers have been tried, and they provide luminance levels of 60 Cd/m^2, and 160 Cd/m^2 within the viewing field.

OCIS codes: (120.2040) Displays; (230.1980) Diffusers; (330.1400) Vision - binocular and stereopsis.

References and links

1. Q. Wang, Y. Tao, W. Zhao, and D. Li, "A full resolution autostereoscopic 3d display based on polarizer parallax barrier" Chinese Optics Letters **8**, 22–23 (2010).
2. H. Baker and Z. Li, "Camera and projector arrays for immersive 3d video" in "Proceedings of the 2nd International Conference on Immersive Telecommunications" (ICST (Institute for Computer Sciences, Social-Informatics and Telecommunications Engineering), 2009), 23.
3. W. Matusik and H. Pfister, "3d tv: a scalable system for real-time acquisition, transmission, and autostereoscopic display of dynamic scenes" ACM Trans. Graph. **23**, 814–824 (2004).
4. P. Harman, "Autostereoscopic teleconferencing system" in "Electronic Imaging," (International Society for Optics and Photonics, 2000), 293–302.
5. K. Aksit, S. Olcer, E. Erden, V. Kishore, H. Urey, E. Willman, H. Baghsiahi, S. Day, D. Selviah, F. Fernandez, and P. Surman, "Light engine and optics for helium3d auto-stereoscopic laser scanning display" in "3DTV Conference: The True Vision - Capture, Transmission and Display of 3D Video (3DTV-CON), 2011" (2011), 1 –4.
6. R. Borner, B. Duckstein, O. Machui, H. Roder, T. Sinnig, and T. Sikora, "A family of single-user autostereoscopic displays with head-tracking capabilities" Circuits and Systems for Video Technology, IEEE Transactions on **10**, 234 –243 (2000).
7. S. S. Kim, S. A. Shestak, K. H. Cha, and J. H. Sung, "Multiview 3d projection system" 222–226 (2004).
8. C. Gao and J. Xiao, "Retro-reflective light diffusing display systems" (2009). US Patent App. 12/418,137.
9. M. Scholl, "Ray trace through a corner-cube retroreflector with complex reflection coefficients" JOSA A **12**, 1589–1592 (1995).
10. I. Microvision, "Microvision: A World of Display and Imaging Opportunities" http://www.microvision.com (2012).
11. O. E. GmbH, "Reflective products - lighting optics, optical engineers, polymer processing - Reflexite" http://www.reflexite.com (2012).
12. L. Luminit, "Luminit, The Light Shaping Diffuser (LSD) Company Luminit Shaping Light as Needed" http://www.luminitco.com (2012).
13. I. Github, "kunguz/osman," https://github.com/kunguz/osman (2012).
14. A. J. Woods, "How are crosstalk and ghosting defined in the stereoscopic literature?" 78630Z–78630Z–12 (2011).

#196625 - $15.00 USD Received 29 Aug 2013; revised 11 Oct 2013; accepted 11 Oct 2013; published 15 Nov 2013

15. F. L. Kooi and A. Toet, "Visual comfort of binocular and 3d displays" Displays **25**, 99 – 108 (2004).
16. P. Harman, "Retroreflective screens and their application to autostereoscopic displays" in "Electronic Imaging'97" (International Society for Optics and Photonics, 1997), 145–153.

1. Introduction

Autostereoscopic displays form at least two exit pupils, through which a three-dimensional (3D) image is observed without glasses. The exit pupils can be either fixed, or can dynamically follow viewer's head position under the control of a head-tracker. A large viewing field for the viewer in an autostereoscopic projection display can be achieved by creating tens of exit pupils using the parallax barrier approach [1], or using an array of projectors [2, 3]. Alternatively, one can design a display tracking the viewer's eye using dynamic exit pupils [4–6]. The main advantage of tracking displays is that full resolution is achieved in each view, but they are typically limited to one or few viewers. Projection based autostereoscopic displays employ various transfer screens to form an exit pupil, such as retro-reflective light diffusing screen [2,4], double lenticular screen [3], or Fresnel lens in front of a light shaping diffuser [5, 7].

In this paper, we propose a novel autostereoscopic projection display technique which employs a transfer screen to form a pair of dynamic vertical viewing slits aligned with the viewer's eyes. Any of the aforementioned transfer screens can be used for the proposed technique. The viewing slits track the viewer's eyes in a large viewing field by rotating the transfer screen in-plane. Advantages of the proposed technique are as follows: it requires only two projectors rather than an array of projectors; there is no image registration problem on the screen due to movement of projectors; the viewing slits always track the viewer, so the viewer never perceives discrete transitions between different perspectives; the technique can provide high-gain, and sufficient brightness even with a pair of mobile projectors. The main limitation of this technique is that it is suitable for only one viewer. Luminance, crosstalk, and dynamic viewing area analysis, and measurement results as well as a video demonstration of the system are presented.

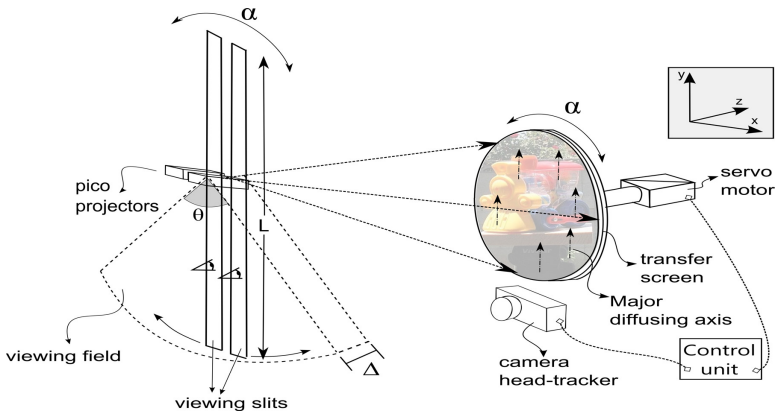

Fig. 1. System sketch showing the elements and the created viewing field of the display.

2. Concept of the display

The system sketch shown in Fig. 1 shows two pico projectors, a rotating transfer screen, an head-tracker unit, and a control unit. The stereo content is projected onto the transfer screen by two pico projectors which are placed horizontally apart from each other by average human interpupillary distance (*IPD*), 63 *mm*. Each projector is assigned to one eye of the viewer. One projector projects the content for the right eye perspective and the other projects the content

#196625 - $15.00 USD Received 29 Aug 2013; revised 11 Oct 2013; accepted 11 Oct 2013; published 15 Nov 2013

for the left eye perspective. On the plane of projectors, as shown in Fig. 1, the transfer screen creates two viewing slits, each of which is parallel to the major diffusing axis of the single axis diffuser, and crosses over the position of corresponding pico projector's micro electromechanical system (MEMS) based scanner. Each viewing slit contains the image content projected by the corresponding pico projector. The creation of viewing slits by by using a retro-reflective diffuser screen, as transfer screen, has been explained in [8]. A viewer, who is standing in the plane of pico projector and looks through the viewing slits, perceives stereo images.

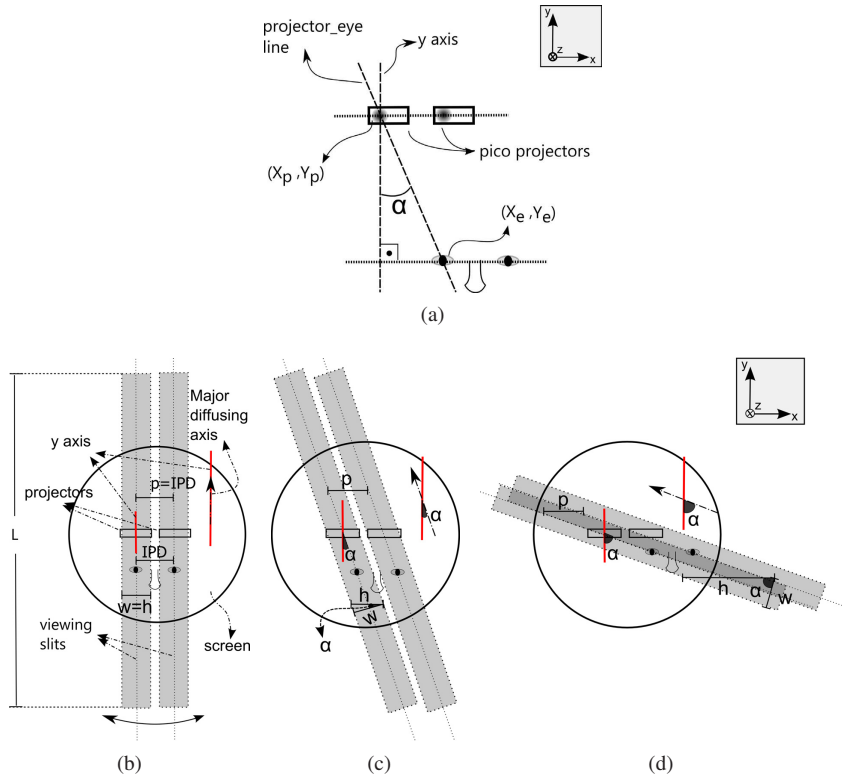

Fig. 2. Viewing slits for different orientations of the transfer screen. (a) Relative angular position of viewer's eyes with respect to projectors (b) Rotation of transfer screen by 0^o of α and $w < 2 \times IPD$, thus $h = w < 2 \times IPD$ (c) Rotation of transfer screen by small α, thus $w < h < 2 \times IPD$ (d) Rotation of transfer screen by large α, thus $h > 2 \times IPD > w$, and there is crosstalk between viewing slits.

$$\alpha = arctan(\frac{X_e - X_p}{Y_e - Y_p}) \tag{1}$$

In order to change the position of viewing slits according to the position of viewer's eyes, a head-tracker unit tracks the position of the viewer, and sends the position information to the control unit. Using the formula of Eq. (1), the control unit calculates the angular position of the viewer, α, which is the angle between eye-projector line and y axis, as shown in Fig. 2(a). Using the angle, α, a servo motor rotates the transfer screen in-plane such that the major diffusing axis of the diffuser makes the same angle with y axis as eye-projector line does, as in Fig. 2. Thus, viewing slits dynamically track the viewer in a large viewing field, as depicted in Fig. 1. The motion of the viewing slits is analogous to the in-plane rotation of a beam around an

#196625 - $15.00 USD Received 29 Aug 2013; revised 11 Oct 2013; accepted 11 Oct 2013; published 15 Nov 2013

anchor point. The MEMS scanner of the pico projector is the anchor point of the corresponding viewing slit.

By projecting different perspective images for the corresponding positions of the viewer, a multi-view 3D display is realized. The proposed technique provides multi-view stereo vision to a single viewer in a large viewing field, which is an arc of a circle with projectors at its center, as depicted in Fig. 1.

3. Characterization of the display

Table 1. Definitions of Symbols

	Parameter	Symbol
Prototype Parameters	Projection Distance	d
	Projection Angle	β
	Screen size	s
	Diffusing angle in major axis (FWHM)	ϕ
	Diffusing angle in minor axis (FWHM)	ψ
	Distance between two projectors	p
	Diameter of projector's MEMS scanner	d_p
	Interpupillary Distance	IPD
Viewing Slits Parameters	Distance between slits	p
	Actual width	w
	Horizontal width	h
	Rotation angle	α
	Length	L
	Maximum rotation angle	θ
	Depth	Δ

The viewing field of the proposed autostereoscopic display technique is characterized by the length, L, depth, Δ, and the maximum rotation angle, θ, of viewing slits, as depicted in Fig. 1. For the proposed technique, the viewing field has been defined as the three-dimensional space in which the crosstalk value of the display is low enough to perceive stereo images.

$$L = 2 \times d \times tan(\phi/2) \tag{2}$$

The length, L, of viewing slits characterizes the luminance of the display across the projector plane. It is determined by the projection distance, d, and diffusing angle, ϕ, of single axis diffuser in major axis, as in Eq. (2). As the viewer moves away from the center of the viewing slit, which is the position of the pico projector, the luminance of the display decreases, according to the diffusing properties of the diffuser. If the diffusing angle, ϕ, is expressed as full-width-at-half-maximum (FWHM) value, then the luminance of the display is less than 50% of the maximum luminance beyond the length, L, of viewing slits.

#196625 - $15.00 USD Received 29 Aug 2013; revised 11 Oct 2013; accepted 11 Oct 2013; published 15 Nov 2013

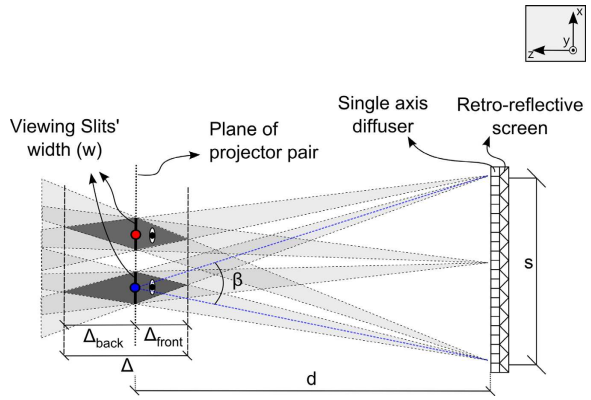

Fig. 3. Top view of the system showing depth of viewing slits.

$$\frac{s}{w} = \frac{d - \Delta_{front}}{\Delta_{front}} = \frac{d + \Delta_{back}}{\Delta_{back}} \tag{3}$$

$$\Delta = \Delta_{front} + \Delta_{back} = \frac{d}{\frac{s}{w} + 1} + \frac{d}{\frac{s}{w} - 1} \tag{4}$$

The depth, Δ, of the viewing slits characterizes the luminance of the display along the projection axis. As the viewer moves away from the projector plane along the projection axis, the luminance decreases at the edges of the transfer screen. Figure 3 illustrates a top view of the proposed system. In Fig. 3, the projection angle of the projector is shown as β, projectors to screen distance is shown as d, the width of viewing slit is shown as w, and the depth of viewing slits is shown as Δ. By using the triangle similarity expressed in Eq. (3), the depth, Δ, of viewing slits can be calculated as in Eq. (4). If the width, w is FWHM value, the luminance at the edges of the transfer screen is less than 50% of the maximum luminance beyond the depth, Δ, of viewing slits.

$$h = \frac{w}{cos(\alpha)} \tag{5}$$

$$h < 2 \times IPD \tag{6}$$

$$\alpha < \theta = arccos(\frac{w}{2 \times IPD}) \tag{7}$$

The maximum rotation angle, θ, of the viewing slits is the rotation angle, α, beyond which the horizontal width of the viewing slits, h, is larger than $2 \times IPD$, as in Fig. 2(d), and crosstalk results in inseparable stereo images. The horizontal width of viewing slits, h, is the full-width-at-zero-intensity (FWZI) width of viewing slits along the horizontal axis, x-axis. In order to avoid crosstalk between stereo images, following two conditions must be satisfied in the proposed system design; (1) the horizontal distance between viewing slits, p must be equal to interpupillary distance of the viewer, IPD, and (2) the horizontal width of viewing slits, h, must be smaller than $2 \times IPD$, as in Figs. 2(b) and 2(c).

The transfer screen does one-to-one imaging to form exit pupils of pico projectors. Placing two projectors horizontally apart from each other by IPD makes the horizontal distance between viewing slits, p, equal to the interpupillary distance of the viewer, IPD. Thus, the

#196625 - $15.00 USD Received 29 Aug 2013; revised 11 Oct 2013; accepted 11 Oct 2013; published 15 Nov 2013

aforementioned first condition to avoid crosstalk is satisfied, as long as the viewer's eyes are aligned along the horizontal axis.

The horizontal width of viewing slits, h, increases with the increase in rotation angle, α, of viewing slits, as seen in Figs. 2(b)-2(d). The relationship between the horizontal width, h, and rotation angle, α, of viewing slits is stated in Eq. (5), where w is the actual width of viewing slits. It is the FWZI width of the viewing slit, which is measured across the viewing slit at right angles of its length. It is a fixed system parameter which is proportional to the projection distance, d, the diffusing angle of single axis diffuser in minor axis, ψ, and the diameter of MEMS scanner of projector, d_p. By placing Eq. (5) into Eq. (6), the second condition to avoid crosstalk, stated in Eq. (6), can be restated as in Eq. (7). Equation (7) implies that there is a maximum rotation angle, α, of viewing slits, beyond which crosstalk results in inseparable stereo images.

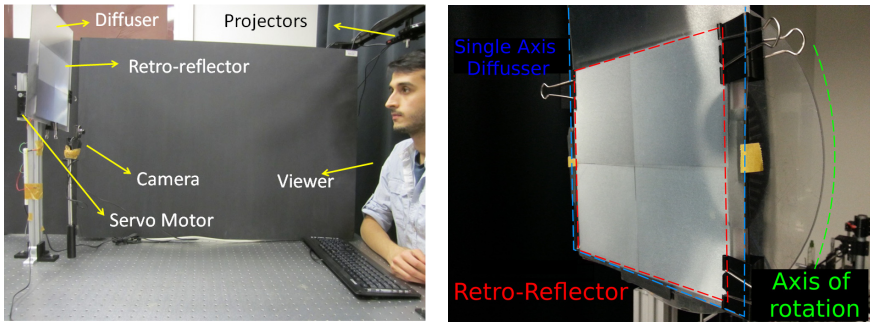

(a) (b)

Fig. 4. (a) The realised prototype. (b) The transfer screen consisting a retro-reflector and a diffuser.

4. The prototype

A prototype was realised to demonstrate the capabilities of the proposed technique. The prototype consists of two MEMS based laser pico projectors from Microvision, Inc. [10], a retro-reflective diffuser screen as a transfer screen [8], an in-house made head-tracker unit [13], an in-house made rotating mechanism which rotates the transfer screen around its center, and a personal computer. Figure 4(a) shows a photograph of the realised prototype.

Table 2. Prototype Parameters

Parameter	Symbol	Value
Projection Distance	d	1180 mm
Projection Angle	β	9.68^o
Screen size	s	200 mm
Diffusing angle in major axis (FWHM)	ϕ	40^o
Diffusing angle in minor axis (FWHM)	ψ	0.2^o
Distance between two projectors	p	63 mm
Diameter of projector MEMS scanner	d_p	1 mm
Diameter of eye pupil	d_{eye}	2 $mm - 8$ mm
Interpupillary Distance	IPD	63 mm

The transfer screen is a layered composition of a retro-reflective sheet [9] from Reflexite [11], and a single axis diffuser (large diffusing angle in major axis and small diffusing angle in the

#196625 - $15.00 USD Received 29 Aug 2013; revised 11 Oct 2013; accepted 11 Oct 2013; published 15 Nov 2013

perpendicular minor axis). Two different types of single axis diffuser have been tested as the diffuser layer of the transfer screen. Diffuser 1 is a randomly patterned aperiodic diffuser from Luminit, LLC [12] with FWHM diffusing angle, ϕ, of 40^0 in major axis, and, ψ of 0.2^0 in minor axis. Diffuser 2 is a conventional periodic diffuser with FWHM diffusing angle, ϕ, of 20^0 in major axis, and, ψ of $\sim 0^0$ in minor axis. The retro-reflector sheet is a high fill factor 200 $mm \times 200$ mm corner cube retro-reflector array with 0.254 mm pitch size. As the screen size is equal to the retro-reflector sheet size, it can be enlarged using an improved mechanical design to support a larger screen. All prototype parameters are presented in Table 2.

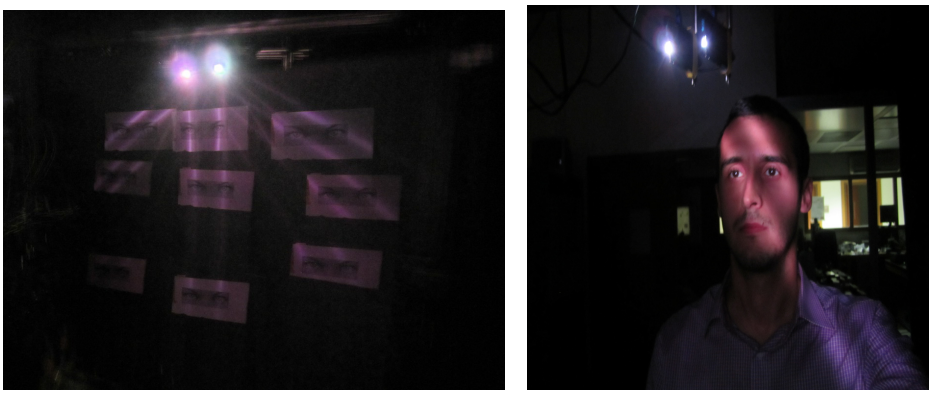

(a) (b)

Fig. 5. (a) Created viewing slits at different rotation angles: 9 shots are superimposed in order to create the photograph. The two bright spots in the photograph are pico projectors. (b) A sample picture of viewer, showing viewing slits on his eyes' position (Media 1: illustrates the head-tracker and screen rotation real-time. Media 2: illustrates right eye and left eye views captured with a camera that moves with the viewer.).

It is enough to rotate only single axis diffuser in order to create dynamic viewing slits. However, in the prototype, rotating mechanism rotates both retro-reflector sheet and the single axis diffuser which makes the realization of the prototype easier. The created viewing field is illustrated in Fig. 5(a) by taking pictures of viewer space for different rotation angles of viewing slits. Figure 5(b) shows a sample picture of viewer while viewing slits appear on his eyes' position.

Specular reflections create two bright lines across the transfer screen, which result in double image along the bright lines. The specular reflections can be eliminated by anti-reflection (AR) coating surfaces, or by tilting the transfer screen around the vertical axis, y-axis. In the prototype, display screen has been tilted by 5^o around the vertical axis, so specular reflections are not observed on the transfer screen. Fig. 6(a) is a picture of the screen taken from the left eye viewing slit. Fig. 6(c) is a picture of the screen taken between left and right eye viewing slits, thus both right and left eye images are observed.

#196625 - $15.00 USD Received 29 Aug 2013; revised 11 Oct 2013; accepted 11 Oct 2013; published 15 Nov 2013

(a) (b) (c)

Fig. 6. Screen shots taken from different viewing positions: (a) left eye, (b) right eye, and (c) between the two eyes. (Media 3) video shows L and R images as a camera is moved laterally within the viewing field.

5. Results and discussions

As a quality measure, a crosstalk analysis of the realized prototype for both diffusers was conducted. The crosstalk has been quantized by Eq. (8), where leakage is the maximum luminance of light that leaks from unintended channel to the intended channel, and 'signal' is maximum luminance of the intended channel, [14].

$$crosstalk(\%) = \frac{leakage}{signal} \times 100 \tag{8}$$

Thus, two luminance measurements of the screen are taken from each eye's position to calculate the crosstalk value of the corresponding eye. In the conducted experiments, only crosstalk values for the left eye has been measured, since the system is approximately symmetrical. For the first luminance measurement, which determines the leakage, full black image is projected by left-eye projector, and full white image is projected by right-eye projector. For the second measurement, which determines the signal, images for the first measurement are swapped. Luminance values have been measured by a calibrated camera from Radiant Imaging, which takes photometrically weighted photographs, and inserted into Eq. (8). By repeating the explained procedure above for different positions of camera in viewer's space, and interpolating the measured values; crosstalk, and luminance maps of viewer's space have been obtained for both transfer screen with diffuser 1, and transfer screen with diffuser 2.

#196625 - $15.00 USD Received 29 Aug 2013; revised 11 Oct 2013; accepted 11 Oct 2013; published 15 Nov 2013

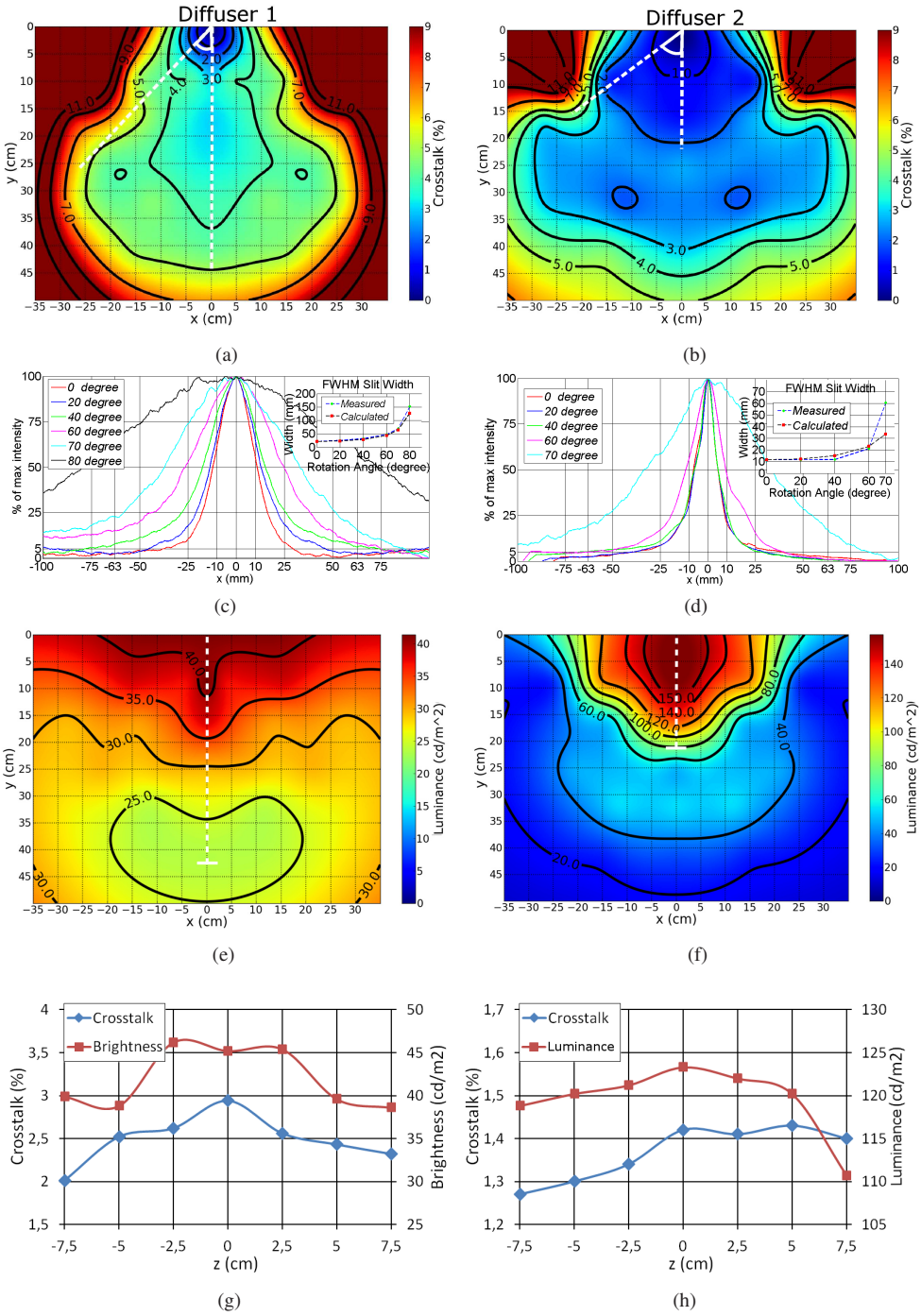

Fig. 7. (a) and (b) Interpolated crosstalk maps of viewer's space at the projector plane for diffusers I and II. (c) and (d) Horizontal cross-sections of viewing slits for different rotation angle, a for diffusers I and II. (e) and (f) Interpolated luminance map of viewer's space at the projector plane for diffuser 1 and 2. (g) and (h) Crosstalk and luminance variations along the projection axis for diffuser 1 and 2 at the position (x,y) = (0,9)cm and z is variable in the measurements.

#196625 - $15.00 USD Received 29 Aug 2013; revised 11 Oct 2013; accepted 11 Oct 2013; published 15 Nov 2013

Figure 7(a) is the obtained crosstalk map of the viewer's space in projector plane for screen with diffuser 1. According to [15], crosstalk should be less than 5 % in order to prevent reduced viewing comfort in half of population. Thus the maximum rotation angle, θ, of viewing slits is 46^o, beyond which the crosstalk is more than 5 %, and results in inseparable stereo images. Figure 7(c) illustrates the horizontal cross-section of viewing slits for different rotation angles. The actual width, *w*, of viewing slits, which is the full width at 5 % of maximum intensity, for 0^o of rotation, is 75 *mm*. By placing the actual width, *w*, of viewing slit into Eq. (7), the maximum rotation angle, θ, of viewing slits is calculated as 53^0, which validates the experimental result of 46^o.

Figure 7(e) is the luminance map of viewer's space in projector plane. The luminance of the display decreases to 50% of the maximum luminance at around 420 *mm* away from the center of viewing slits, which are located at (0,0) in coordinate system. Thus, the FWHM length, *L*, of viewing slits is 840 *mm*. By placing the prototype parameters, stated in Table 2, into Eq. (2), the FWHM length, *L*, of viewing slits is calculated as 859 *mm*, which validates the experimental result of 840 *mm*.

Figure 7(g) shows the crosstalk, and luminance variations in projection axis. The crosstalk of the display is below 5 % for ± 7.5 *cm* away from the projector plane. Thus, the viewer still perceives stereo images away from the projector plane. However, as the viewer moves away from the projector plane, perceived luminance varies over the transfer screen.

In order to increase the viewing field by increasing the maximum rotation angle, θ, of viewing slits, another transfer screen has been constructed by replacing diffuser 1, $40^o \times 0.2^o$ aperiodic single axis diffuser, with diffuser 2, $20^o \times 0^o$ periodic diffuser. Crosstalk, and luminance maps of the viewer's space have been obtained for the screen with diffuser 2, and presented in Figs. 7(b), 7(f), and 7(h). The crosstalk of the screen with diffuser 2 is less than the diffuser 1, for the same area of viewer's space, as presented in Fig. 7(a). The maximum rotation angle, θ, of viewing slits is 58^o for the prototype 2, and it is more than the maximum rotation angle, θ, of viewing slits for the diffuser 1, which is 46^o. Figure 7(d) illustrates the horizontal cross-section of viewing slits for different rotation angles. As seen in Fig. 7(d), the actual width, *w*, of viewing slits, which is the full width at 5 % of maximum intensity for 0^o of rotation, is around 60 *mm*. By placing the actual width, *w*, of viewing slit into Eq. 7, the maximum rotation angle, θ, of viewing slits is calculated as 61^o, which validates the experimental result of 58^o.

Figure 7(f) is the luminance map of viewer's space in projector plane for the the screen with diffuser 2. As seen in Fig. 7(f), the luminance of the display decreases to 50% of the maximum luminance at around 210 *mm* away from the center of viewing slits. Thus, the FWHM length, *L*, of viewing slits is 420 *mm*. By placing the prototype 2 parameters, which are the projection distance, *d*, of 1180 *mm*, and the FWHM diffusing angle, ϕ, of 20^o into Eq. (2), the FWHM length, *L*, of viewing slits is calculated as 416 *mm*, which validates the experimental result of 420 *mm*.

Figure 7(h) shows the crosstalk, and luminance variations in projection axis for the screen with diffuser 2. The crosstalk for the diffuser 2 is less than the crosstalk for diffuser 1, for ± 7.5 *cm* away from the projector plane, as presented in Fig. 7(g)

As the periodic diffuser is used instead of aperiodic diffuser, the crosstalk of the display in viewer's space has decreased significantly. However, the mismatch between the periodicity of retro-reflector sheet, and the periodicity of single axis diffuser created Moiré patterns on transfer screen, as seen in Fig. 8(a). Thus, the single axis diffuser must be aperiodic in order to have a Moiré-free transfer screen, as seen in Fig. 8(b). Although the periodic diffuser creates Moiré patterns, subjects have stated that the display presents successful stereoscopic vision for both types of the single axis light diffuser.

#196625 - $15.00 USD Received 29 Aug 2013; revised 11 Oct 2013; accepted 11 Oct 2013; published 15 Nov 2013

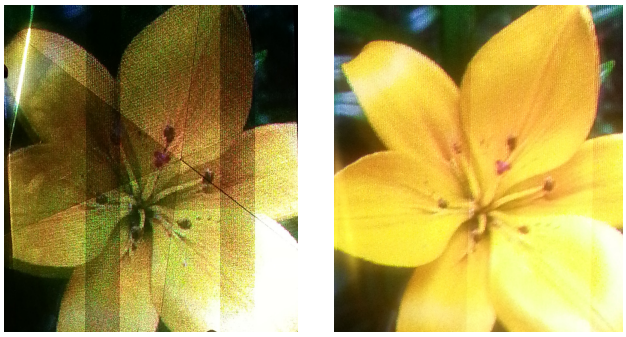

(a) (b)

Fig. 8. Images captured from a screen with (a) periodic and (b) aperiodic diffuser, respectively. Moire artefacts are visible in the periodic screen.

In projection-based displays, screen size, s, is determined by the projection distance, d, and the projection angle, β, as in Eq. 9. For the displays which project images on Lambertian scattering surfaces, the screen size, s, is limited by the projector's power, since as the projection distance, d, increases, the luminance of the display decreases dramatically.

$$s = 2 \times d \times tan(\beta/2) \tag{9}$$

As the screen in prototype is a high gain retro-reflective diffusing surface, all generated power is concentrated into the viewing slits, and luminance is always reasonably high in the viewing slits regardless of projection distance. Retro-reflective surfaces can have gains of between $1k - 10k$ [16]. Thus, projection distance, d, and screen size, s, is not limited by the projector power. However, it should also be noted that, as the retro-reflector screens work under a specific acceptance angle limit, projection angle, β can not exceed the acceptance angle limit. In the prototype, projection angle, β, is $9,68^o$, which is smaller than the acceptance angle, 30^o, of retro-reflector.

6. Conclusion

A new type of multi-view autostereoscopic projection display, using a pair of MEMS scanner based pico projectors, a head-tracking camera, and a rotating retro-reflective diffuser screen is proposed and demonstrated. Analytical and experimental results for crosstalk and luminance are in good agreement. The screen with diffuser 1 achieved a viewing field of 500 *mm* in horizontal axis, and 450 *mm* in vertical axis. The screen with diffuser 2 achieved a viewing field of 700 *mm* in horizontal axis, and 500 *mm* in vertical axis. The crosstalk of the display is below 5 % for both diffusers. The maximum luminance of the display is 50 cd/m^2 and 160 cd/m^2 for diffuser 1 and diffuser 2, respectively. The crosstalk remained below 5 % within ± 7.5 *cm* in the z-axis, i.e., user can move back and forth about 15 *cm* and the crosstalk remain at acceptable levels while the luminance dropped by 25 % and 10 % for Screen 1 and Screen 2. Beyond that range, the luminance at the edges of the transfer screen decreases and corners of the images are vignetted.

The technique introduced in this paper provides a large-screen autostreoscopic projection display using a pair of low-lumen projectors for a single viewer. Full resolution of the display is maintained. Retro-reflective screen provides high brightness gain. The transition between different perspectives is smooth as viewing slits track the eyes real-time. Some of main applications are personal entertainment displays used in cars, planes, and simulators.

#196625 - $15.00 USD Received 29 Aug 2013; revised 11 Oct 2013; accepted 11 Oct 2013; published 15 Nov 2013

Acknowledgment

This research is sponsored by The Scientific and Technological Research Council of Turkey (TÜBİTAK), Project No: 111E183.

#196625 - $15.00 USD Received 29 Aug 2013; revised 11 Oct 2013; accepted 11 Oct 2013; published 15 Nov 2013